# Snake Robot Shape Sensing Using Micro-inertial Sensors

Zhiqiang Zhang, Jianzhong Shang, Carlo Seneci and Guang-Zhong Yang *Fellow, IEEE*

*Abstract*— Real-time shape sensing and state acquisition is important for closed-loop control of hyper-redundant snake robots in minimally invasive surgery. Due to the miniaturized size of such minimally invasive surgery robots, it is not feasible to use existing angular sensors involving rotary encoders. With recent advances of the MEMS technology, micro inertial sensors have shown their potential for robot state estimation. Previous studies have demonstrated that accurate joint angles can be estimated for one degree-of-freedom (DoF) joints. However, higher DoF joints of the robot can impose a number of challenges to the current joint angle estimation methods. This paper presents a micro-sensing platform and shape reconstruction algorithm for minimally invasive surgery snake robot with two DoF joints. The method incorporates both gravitational and gyroscopic sensing for calculating the rotation difference between any consecutive robot segments. The gyroscope measurements are first used as the input to predict the rotation difference by direct orientation integration. The orientation difference is then derived from the consecutive acceleration vectors to update the prediction through a complementary filter. To demonstrate the performance of our proposed approach, a robot prototype with two universal joints was fabricated. Detailed experimental results have demonstrated that high accuracy can be achieved by using the proposed method for joint angle estimation.

## I. INTRODUCTION

Robotic assisted surgery is a rapidly expanding field in recent years, with a wide range of robot platforms being developed. To cater for emerging surgical techniques such as single incision laparoscopic surgery and natural orifice trans-luminal endoscopic surgery, many snake-like hyper-redundant robots have been proposed [1]–[3]. When these robots are operated under a master-slave setup, real-time proprioceptive position feedback is not essential as human vision and manipulation is used to close the control loop. However, when reconstructing the snake robot shape, position feedback is critical. In general, snake-like surgical robots can be divided into two categories: tendon actuated continuum robots and articulated joint based robots. Tendon actuated continuum robots usually use the tendon displacement at the proximal end where the actuators are located to control the posture of the robot [4]. Large errors can be caused due to robot shape deformation or backlash of the robot. Recent development of fibre optic shape sensing provides a new way of reconstructing the shape of the robot, but application of such technology to snake robots is still in its infancy. For joint based robots, the most common sensing element used currently is rotary encoders, which provide precise angular displacement. Recently, we have developed an articulated

Z. Zhang, J. Shang, C. Seneci, G.-Z. Yang are with the Hamlyn Centre for Robotic Surgery, Imperial College London, UK {z.zhang, j.shang, c.seneci, g.z.yang} at imperial.ac.uk

universal joint based snake-like robot for minimally invasive surgery [3]. The need for size miniaturization of the robot for minimally invasive surgery procedures means it is not feasible to use the traditional rotary encoders. The purpose of this work is to explore a new way of sensing the joint angles based on micro-inertial sensors.

Thus far, micro-inertial sensors have been extensively used for wearable human motion estimation. The wearable inertial sensors can be placed on strategic locations of the human body to derive motion information of each link, so that the overall posture of the body can be reconstructed, typically with a constraint kinematic model [5] [6]. Due to the inherent drift of the inertial sensor, other micro-sensors such as magnetometer, are used in parallel to counteract the problem of drift [7] [8]. Some commercial products for body-posture reconstruction are already available on the market [9] [10] and they have been used not only for human biomechanical analysis [11] and activity recognition [12], but also for virtual reality and navigation [13] [14].

Previous work of using inertial sensors in robotic manipulation is mainly focused on kinematic calibration and fault detection. Inertial sensors can offer a compelling source of information [15] [16], but none of them has attempted for robot state estimation and control. Recently, some research effects have demonstrated that it is possible to estimate robot joint angles using inertial sensors. For example, Ghassemi et al. [17] designed and implemented an angle sensing method for a mini-excavator arm, and the approach was based on processing the outputs of a pair of biaxial accelerometers placed close to the joint axis on the adjacent links. Quigley et al [18] explored the use of consumer-grade accelerometers as joint position sensors for robotic manipulators, and they presented an extend Kalman filter (EKF) based method to infer the joint angles from a 3-d accelerometer mounted on each pair of joints. Roan et al. [19] presented a strategy for angular position estimation of revolute joints in rigid bodies using micro-accelerometers and gyroscopes. Common filtering techniques were adapted to combine the joint angles estimated from one triaxial accelerometer on each link and the measurements from a uniaxial gyroscope. However, all methods mentioned above were designed only for one degree-of-freedom (DoF) joint angle estimation. For robots with higher DoFs, however, there are many practical difficulties for accurate joint angles estimation due to more flexibility of the robot movement.

The aim of this paper is to propose a new joint angle estimation scheme for hyper-redundant robots with two DoF joints. The method incorporates a triaxial accelerometer and a triaxial gyroscope on each link to calculate the rotation
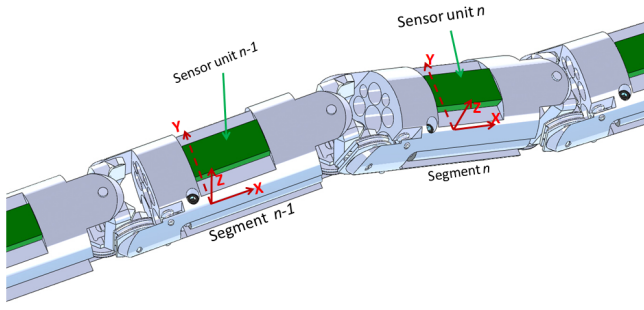
Fig. 1. Schematic illustration of segment $n-1$ and segment $n$ in a snake robot. An inertial sensor unit (green cuboid) consisting of a three-axes accelerometer and gyroscope is mounted onto each segment. The local segment coordinate system is defined as shown in the figure. The joint between segment $n-1$ and $n$ for example, can have two DoFs: rotating around $Z$ axis of segment $n-1$ and rotating around $Y$ axis of segment $n$.

difference between any consecutive robot segments. The gyroscope measurements are used as the input for direct orientation integration and prediction of the rotation difference between adjacent robot segments. The consecutive acceleration vectors are also used to derive the orientation difference and update the gyroscope prediction through a complementary filter. To demonstrate the performance of our proposed approach, a robot prototype with universal joints was fabricated. The experimental results have demonstrated that our proposed method can achieve accurate joint angle estimation when compared to the ground-truth data.

## II. METHODS

The main objective of the proposed joint state estimation scheme is to recursively estimate the orientation of each robot segment from the stationary robot base to the final manipulator. Here we use quaternion to represent the segment orientation due to its computational efficiency and free of singularity. Fig 1 gives a schematic illustration of the segment $n-1$ and segment $n$ of a snake robot. A sensor unit is mounted on each segment. The robot shape sensing is to estimate the orientation $q_t^n$ of segment $n$ at time $t$ from the $n^{th}$ sensor unit measurement $y_t^n$ and and $(n-1)^{th}$ sensor measurement $y_t^{n-1}$ given the segment $n-1$ orientation $q_t^{n-1}$.

Three coordinate systems are used in our method: 1) the global coordinate system used as the reference; 2) the sensor coordinate system with the axes aligned with the inertial sensor unit; 3) the robot segment coordinate system for the local coordinate system of each robot segment. For the rest of this paper, we will use capital $X$, $Y$ and $Z$ to represent the axes of coordinate systems. The robot segment coordinate system is defined as: X pointing towards the longitudinal direction, Y pointing backwards while Z pointing upwards to construct a right hand system. For the joint between segment $n-1$ and $n$ for example, it can have two DoFs incorporating rotation around $Z$ axis of segment $n-1$ and rotation around $Y$ axis of segment $n$.

For any sensor unit $n$, the sensor unit measurement $y_t^n$ consists of two parts: 3-axis accelerometer measurement

$y_{a,t}^n = [y_{a,t}^{n,X}, \ y_{a,t}^{n,Y}, y_{a,t}^{n,Z}]$ and gyroscope measurement $y_{g,t}^n = [y_{g,t}^{n,X}, \ y_{g,t}^{n,Y}, y_{g,t}^{n,Z}]$. However, we will use the accelerometer measurement only as the gravity component while ignoring the small centripetal and centrifugal components due to the relatively slow movement of the robot. Before processing any sensor measurement, the sensor data needs to be transformed to the local robot segment coordinate system, which can be achieved by the sensor to segment calibration before the snake robot assembling. Here, we assumed that the sensor coordinate system and the local robot segment coordinate system are consistent with each other after calibration.

### A. Gyroscope Prediction

The gyroscope measures the angular rate, so the orientation of segment $n$ can be predicated via the gyroscope signal integration. Given the $n$ segment orientation $q_{t-1}^n$ at time $t-1$, the predicated quaternion can be written as [20]:

$$q_{t|t-1}^n = \Theta_t q_{t-1}^n \tag{1}$$

where $\Theta_t = \exp\{\frac{1}{2}\mathcal{R}(y_{g,t}^n)\Delta t\}$, $\Delta t$ is the sampling rate (we set to 0.03s in our implementation), and $\mathcal{R}(y_{g,t}^n)$ is a $4 \times 4$ skew symmetric matrix as:

$$
\mathcal{R}(y_{g,t}^n) = \begin{bmatrix} -\lfloor y_{g,t}^n \times \rfloor & y_{g,t}^n \\ -\left(y_{g,t}^n\right)^T & 0 \end{bmatrix}
$$
$$
= \begin{bmatrix} 0 & -y_{g,t}^{n,Z} & y_{g,t}^{n,Y} & y_{g,t}^{n,X} \\ y_{g,t}^{n,Z} & 0 & -y_{g,t}^{n,X} & y_{g,t}^{n,Y} \\ -y_{g,t}^{n,Y} & y_{g,t}^{n,X} & 0 & y_{g,t}^{n,Z} \\ -y_{g,t}^{n,X} & -y_{g,t}^{n,Y} & -y_{g,t}^{n,Z} & 0 \end{bmatrix}. \tag{2}
$$

and $\lfloor y_{g,t}^n \times \rfloor$ represent the cross product operator. Based on quaternion integration, $\Theta_t$ can be simplified as:

$$
\Theta_t = \cos\left(\frac{|y_{g,t}^n|\Delta t}{2}\right) \cdot I_{4\times 4} + \frac{1}{|y_{g,t}^n|}\sin\left(\frac{|y_{g,t}^n|\Delta t}{2}\right) \cdot \mathcal{R}(y_{g,t}^n). \tag{3}
$$

The predicted orientation difference $\Delta q_{t|t-1}^{n-1|n}$ between segment $n$ and segment $n-1$ can be written as:

$$\Delta q_{t|t-1}^{n-1|n} = \left(q_{t|t-1}^n\right)^{-1} \otimes q_t^{n-1} \tag{4}$$

where $\otimes$ is the quaternion multiplication. To convert the orientation difference $\Delta q_{t|t-1}^{n-1|n}$ to the rotational angles, the DCM (Direction Cosine Matrix) representation $C(\Delta q_{t|t-1}^{n-1|n})$ of $\Delta q_{t|t-1}^{n-1|n}$ is required:

$$C(\Delta q_{t|t-1}^{n-1|n}) = (q_4^2 - e^T e)I_{3\times 3} + 2ee^T - 2q_4\lfloor e\times \rfloor \tag{5}$$

where $q_4$ and $e$ are the scale and vector parts, respectively, in the quaternion $\Delta q_{t|t-1}^{n-1|n}$ respectively, and the $I_{3\times 3}$ is the identity matrix of dimension $3 \times 3$. The rotation matrix $C(\Delta q_{t|t-1}^{n-1|n})$ can also be represented by Euler angle $\theta_{t|t-1,X}^{n-1|n}$, $\theta_{t|t-1,Y}^{n-1|n}$, $\theta_{t|t-1,Z}^{n-1|n}$, called roll, pitch, yaw, indicating the rotation angle about the $X$, $Y$, $Z$ axes of the $n$ segment

coordinate respectively (XYZ Euler angle is used here. After rotations about $X$ and $Y$ axes of the segment $n$, the $Z$ axes of both the segment $n$ and $n-1$ points the same direction). Based on Euler theory, the three Euler angles or the predicted joint rotation angles can be written as:

$$\theta_{t|t-1,X}^{n-1|n} = atan(c_{32}/c_{33})$$
$$\theta_{t|t-1,Y}^{n-1|n} = atan\left(-c_{31}/\sqrt{c_{11}^2 + c_{21}^2}\right) \quad (6)$$
$$\theta_{t|t-1,Z}^{n-1|n} = atan(c_{21}/c_{11})$$

where $c_{ij}$ is the element of $C(\Delta q_{t|t-1}^{n-1|n})$ at row $i$ and column $j$, and $i, j = 1, 2, 3$.

### B. Acceleration Decomposition

Due to inevitable drift of inertial sensor, any error in $y_{g,t}^n$ can make the error of predicted joint angles increase exponentially; therefore, we use the gravity information to compensate for the drift. Given the accelerometer measurement $y_{a,t}^{n-1}$ and $y_{a,t}^n$ for the segment $n$ and $n-1$, the purpose of the acceleration decomposition is to derive the joint angles from the difference between $y_{a,t}^{n-1}$ and $y_{a,t}^n$. As shown in the Fig. 2, the rotation difference between segment $n$ and $n-1$ can decompose as two simple rotations: 1) Rotate the segment $n$ local coordinate system around its $Y$ axis to form an intermediate coordinate system; and 2) Rotate the intermediate coordinate system around its $Z$ axis to the segment $n-1$ local body coordinate. Thus the acceleration vector $y_{a,t}^{n-1|n} = [y_{a,t}^{n-1|n,X}, \; y_{a,t}^{n-1|n,Y}, \; y_{a,t}^{n-1|n,Z}]^T$ in the intermediate coordinate system should have the following equations:

$$y_{a,t}^{n-1|n,Y} = y_{a,t}^{n,Y}$$
$$y_{a,t}^{n-1|n,Z} = y_{a,t}^{n-1,Z} \quad (7)$$
$$y_{a,t}^{n-1|n,X} = \pm\sqrt{g_0^2 - (y_{a,t}^{n-1|n,Y})^2 - (y_{a,t}^{n-1|n,Z})^2}$$

where $g_0$ is the magnitude of the gravity. Define the joint angles estimation by accelerometers as: $\theta_{t|a,X}^{n-1|n}$, $\theta_{t|a,Y}^{n-1|n}$ and
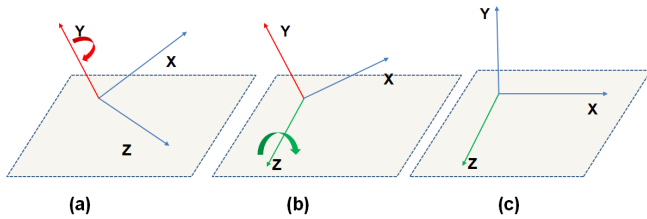


(a)    (b)    (c)

Fig. 2. Schematic illustration of the relative rotation between segment $n-1$ and segment $n$. (a) The segment $n$ local body coordinate system; (b)The intermediate coordinate system after rotating the segment $n$ local coordinate system around its $Y$ axis; (c) The segment $n-1$ local body coordinate system, which is achieved by rotating the intermediate coordinate system around its $Z$ axis.

$\theta_{t|a,Z}^{n-1|n}$, then we can have the following properties:

$$\theta_{t|a,X}^{n-1|n} = 0$$

$$\begin{bmatrix} y_{a,t}^{n-1|n,X} \\ y_{a,t}^{n-1|n,Y} \\ y_{a,t}^{n-1|n,Z} \end{bmatrix} = \begin{bmatrix} cos(\theta_{t|a,Z}^{n-1|n}) & -sin(\theta_{t|a,Z}^{n-1|n}) & 0 \\ sin(\theta_{t|a,Z}^{n-1|n}) & cos(\theta_{t|a,Z}^{n-1|n}) & 0 \\ 0 & 0 & 1 \end{bmatrix} \begin{bmatrix} y_{a,t}^{n-1,X} \\ y_{a,t}^{n-1,Y} \\ y_{a,t}^{n-1,Z} \end{bmatrix}$$

$$\begin{bmatrix} y_{a,t}^{n,X} \\ y_{a,t}^{n,Y} \\ y_{a,t}^{n,Z} \end{bmatrix} = \begin{bmatrix} cos(\theta_{t|a,Y}^{n-1|n}) & 0 & -sin(\theta_{t|a,Z}^{n-1|n}) \\ 0 & 1 & 0 \\ sin(\theta_{t|a,Y}^{n-1|n}) & 0 & cos(\theta_{t|a,Y}^{n-1|n}) \end{bmatrix} \begin{bmatrix} y_{a,t}^{n-1|n,X} \\ y_{a,t}^{n-1|n,Y} \\ y_{a,t}^{n-1|n,Z} \end{bmatrix}$$

$$(8)$$

Thus the joint angles estimated by accelerometers can be written as:

$$\theta_{t|a,X}^{n-1|n} = 0$$
$$\theta_{t|a,Y}^{n-1|n} = atan\left(\frac{y_{a,t}^{n-1|n,Z} y_{a,t}^{n,X} - y_{a,t}^{n-1|n,X} y_{a,t}^{n,Z}}{y_{a,t}^{n-1|n,X} y_{a,t}^{n,X} + y_{a,t}^{n,Z} y_{a,t}^{n-1|n,Z}}\right) \quad (9)$$
$$\theta_{t|a,Z}^{n-1|n} = atan\left(\frac{y_{a,t}^{n-1|n,Y} y_{a,t}^{n-1,X} - y_{a,t}^{n-1|n,X} y_{a,t}^{n-1,Y}}{y_{a,t}^{n-1|n,X} y_{a,t}^{n-1,X} + y_{a,t}^{n-1|n,Y} y_{a,t}^{n-1,Y}}\right)$$

In the above equation (9), only the magnitude of $y_{a,t}^{n-1|n,X}$ is known while the sign of it is still unknown. However, we can use the gyroscope prediction to determine the sign of this variable. Given the predicted $Z$ axis rotation angle $\theta_{t|t-1,Z}^{n-1|n}$, the predicted intermediate acceleration vector $y_{a,t|t-1}^{n-1|n}$ can be written as:

$$y_{a,t|t-1}^{n-1|n} = \begin{bmatrix} y_{a,t|t-1}^{n-1|n,X} \\ y_{a,t|t-1}^{n-1|n,Y} \\ y_{a,t|t-1}^{n-1|n,Z} \end{bmatrix}$$
$$= \begin{bmatrix} cos(\theta_{t|t-1,Z}^{n-1|n}) & -sin(\theta_{t|t-1,Z}^{n-1|n}) & 0 \\ sin(\theta_{t|t-1,Z}^{n-1|n}) & cos(\theta_{t|t-1,Z}^{n-1|n}) & 0 \\ 0 & 0 & 1 \end{bmatrix} \begin{bmatrix} y_{a,t}^{n-1,X} \\ y_{a,t}^{n-1,Y} \\ y_{a,t}^{n-1,Z} \end{bmatrix} \quad (10)$$

Therefore the sign of $y_{a,t}^{n-1|n,X}$ can be selected as:

$$sign(y_{a,t}^{n-1|n,X}) = \begin{cases} 1, & if \quad y_{a,t|t-1}^{n-1|n,X} \geq 0 \\ -1, & if \quad y_{a,t|t-1}^{n-1|n,X} < 0 \end{cases} \quad (11)$$

### C. Complementary Filter

The complementary filter is chosen to combine the gyroscope prediction and acceleration decomposition result for joint angle estimation due to its simplicity and efficiency. The acceleration decomposition normally introduces high frequency noise, whereas the drift in the gyroscope prediction is primarily low frequency. A simple complementary filter is designed by passing the acceleration decomposition results and the gyroscope prediction through a low-pass filter and a high-pass filter respectively. Using the first-order IIR filters with the same cut-off frequency, the following joint angles

estimation can be derived:

$$\hat{\theta}_{t,X}^{n-1|n} = 0$$
$$\hat{\theta}_{t,Y}^{n-1|n} = \alpha\theta_{t|t-1,Y}^{n-1|n} + (1-\alpha)\theta_{t|a,Y}^{n-1|n} \quad (12)$$
$$\hat{\theta}_{t,Z}^{n-1|n} = \beta\theta_{t|t-1,Z}^{n-1|n} + (1-\beta)\theta_{t|a,Z}^{n-1|n}$$

where $\alpha$ and $\beta$ are smoothing constants which determine the cutoff frequency. In this paper, both of them were set to 0.5 except the following two situations when singularity exists in the acceleration decomposition:

$$\begin{cases} \alpha = 1, & if \quad \left|\|y_{a,t}^{n,Y}\| - g_0\right| < \delta \\ \beta = 1, & if \quad \left|\|y_{a,t}^{n-1,Z}\| - g_0\right| < \delta \end{cases} \quad (13)$$

where $\delta$ is a constant to implicate whether the rotations in Fig. 2 are about the gravity. Once the joint rotation angles are determined as given in equation (12), the $\Delta\hat{q}_t^{n-1|n}$ can be updated by converting the Euler angles to quaternion. Therefore, the final orientation for segment $n$ can be written as:

$$\hat{q}_t^n = q_t^{n-1} \otimes \left(\Delta\hat{q}_t^{n-1|n}\right)^{-1} \quad (14)$$

The whole algorithm is summarized in Algorithm. 1.

---

**Algorithm 1** Joint angles estimation from stationary segment 0 (Base) to N (Manipulator)

---

**Initialization:**
  **for** $n = 0$ to $N$ **do**
    ●Set the initial quaternion for segment $n$: $q_0^n$;
  **end for**
**Angles Estimation:**
  **for** $t = 1, 2, \cdots$ **do**
    ● Set the quaternion of the base to $q_t^0 = q_0^0$ and set the acceleration measurement of the base to $y_{a,t}^0 = y_{a,0}^0$;
    **for** $n = 1$ to $N$ **do**
      ● Use the gyroscope measurements to predict the delta quaternion $\Delta q_{t|t-1}^{n-1|n}$ between the segment $n$ and segment $n-1$;
      ● Calculate the predicted joint angles: $\theta_{t|t-1,X}^{n-1|n}$, $\theta_{t|t-1,Y}^{n-1|n}$ and $\theta_{t|t-1,Z}^{n-1|n}$;
      ● Calculate joint angles by acceleration decomposition: $\theta_{t|a,X}^{n-1|n}$, $\theta_{t|a,Y}^{n-1|n}$ and $\theta_{t|a,Z}^{n-1|n}$;
      ● Update the joint angles estimation by complementary filter: $\hat{\theta}_{t,X}^{n-1|n}, \hat{\theta}_{t,Y}^{n-1|n}, \hat{\theta}_{t,Z}^{n-1|n}$;
      ● Update both the Delta quaternion $\Delta q_t^{n-1|n}$ and the orientation for segment $q_t^n$.
    **end for**
  **end for**

---

## III. EXPERIMENTAL RESULTS

### A. Experimental Setup

To demonstrate the accuracy of using inertial sensors to sense the robot joint angles, a robot prototype with two universal joints was fabricated. This is shown in Fig. 3. The
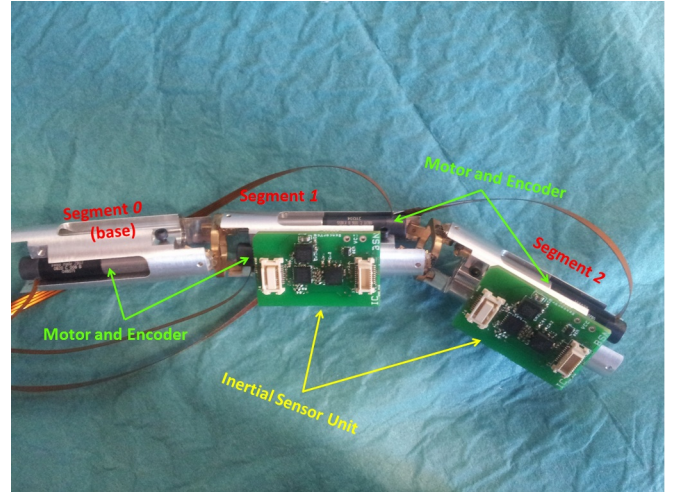


Fig. 3. The fabricated robot prototype with two universal joints

configuration is the same as the robot mentioned in [3]. The design was scaled up in order to be able to fit motors for driving the joints and integrated encoders to measure the joint angles. The integrated quadrature encoder gives 75000 counts per turn, representing resolution of 0.005 degrees, which was used as the ground-truth of the joint angle. The base segment was fixed on a table, while a Body Sensor Network (BSN) sensor node [21] was fixed at the body of each segment. Each BSN node used is equipped with an Analog Devices ADXL330 [22] for 3D acceleration measurement, an InvenSense ITG-3200 digital gyroscope [23] for 3D angular velocity measurement.
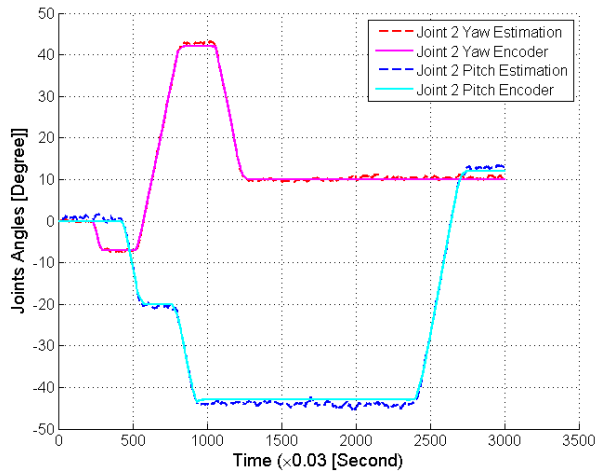
### B. Performance Analysis

At the beginning of each experiment, we manually adjusted the segments 0 and 1 to make them in a straight line, thus we took the acceleration reading on the segment 1 as the acceleration vector $y_{a,0}^0$. During the experiment, the only unknown parameter in our algorithm is $\delta$, which indicates whether the rotation axis is parallel or close to the gravity direction. In our implementation, the $\delta$ was empirically set to $0.28g_0$ to provide the best results based on 10 different trials. In our experiments, the snake-robot was driven smoothly through different trajectories while the

TABLE I

THE RMS, MEAN, SD, MAX ERROR AND CORRELATION COEFFICIENTS OF THE ESTIMATED ANGLES COMPARED TO THE ENCODER.

| | Unit: Degree | | | Correlation |
| | RMS | Mean±SD | Max Error | Coefficient |
|---|---|---|---|---|
| Joint 1: Yaw | 0.4764 | 0.2651±0.3823 | 1.0636 | 0.9999 |
| Joint 1: Pitch | 1.1746 | 0.4446±0.8387 | 3.2003 | 0.9991 |
| Joint 2: Yaw | 0.4000 | -0.0150±0.3890 | 1.2893 | 0.9998 |
| Joint 2: Pitch | 1.2283 | -1.634±0.8269 | 2.7855 | 0.9998 |

(a) Joint 1 Angles
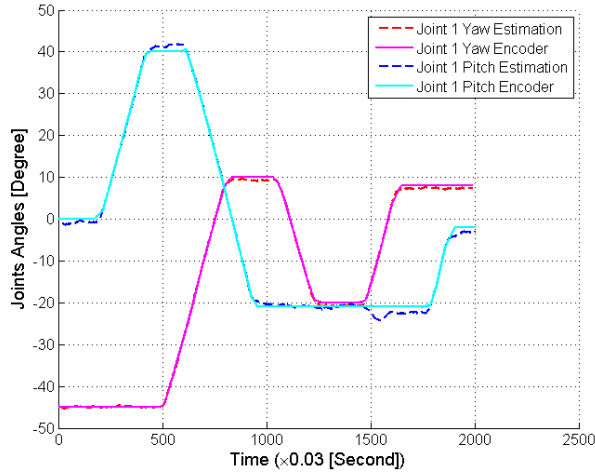

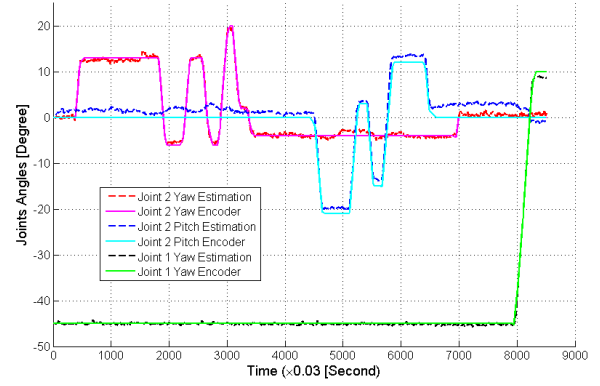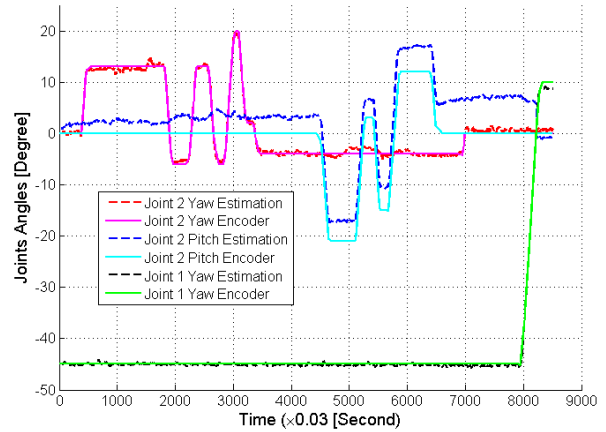
(a) Without Simulated Bias



(b) Joint 2 Angles

Fig. 4. The joint angles estimation and the ground-truth from the on-board quadrature encoders. All the estimation for the 4 joint angles are very close to the corresponding ground-truth.



(b) With Simulated Bias

Fig. 5. Assessment of the robustness of the proposed algorithm. When the one rotation axis (corresponding to pitch angle) of the joint 2 is parallel the gravity for long period, the gyroscope integration will result in drift, which can be removed once the acceleration measurement is back. (a): Integration with the original gyroscope measurements; (b): integration after manually added bias to the gyroscope measurements

inertial sensor units sampled the movement at a rate of 33 Hz. The joint angle readings from the on-board quadrature encoders were compared against the joint angles estimate from the complimentary filter using the accelerometers and gyroscopes.

Figures 4 shows the tracking performance of our proposed method. It is obvious that the error between our estimation and the ground-truth are very small. Table I summarizes the quantitative comparison results between our estimated angles and the ground-truth. In this table, we considered the root mean square error (RMS), mean error, error standard deviation and maximum absolute error between them. Correlation coefficient is also considered. From the results derived, it is evident our proposed method can be used to estimate the robot joint angles accurately.

## C. Error Recovery for Rotations Perpendicular to Gravity

It is wellknown that when the joint motion is in perpendicular to the gravity vector, accelerometer fails to correct the gyro integration drift. In this case, the joint angles cannot be accurately estimated. To further investigate the robustness of the proposed algorithm and accuracy of the proposed method under such condition, we applied the proposed algorithm to extreme operating conditions of the robot. In this experimental, the $Y$ axis of the segment two was set parallel to the gravity, so the pitch angle of the joint 2 can only rely on the gyroscope measurement. After about 240s, we rotated the segment one to make the $Y$ axis of the segment two leave the gravity direction. To make the situation even worse, we added a small bias to all the gyroscope measurement of the sensor unit two to make the integration drift larger. Fig 5 shows the estimated angles. As we can see from the figure, the yaw angle of the joint 2 is resilient to such manually added bias, it is mainly because the angle derived from accelerometer decomposition can compensate for such drift.

Unlike the yaw angle, the pitch angle starts to accumulate drift since there is no acceleration compensation, but once the rotation axis is not close to the gravity direction, the drift can be removed and get accurate estimation.

## IV. CONCLUSION AND FUTURE WORK

In this paper, we have proposed a novel joint angle estimation scheme for snake robot with 2 DoF joints. The gyroscope measurements were used as the input for direct orientation integration and prediction of the rotation difference between adjacent robot segments. The consecutive acceleration vectors were also used to derive the orientation difference and update the gyroscope prediction through a complementary filter. The experimental results derived have demonstrated that the proposed method can achieve accurate joint angle estimation with regards to the on-board quadrature encoder measurements as the ground-truth.

With recent advances in MEMS technology, micro gyroscopes and accelerometers are small enough to be embedded directly into the robot body. It is expected that this will initiate many new engineering opportunities for the mechatronic design of medical robots. By integrating the micro inertial sensors and using the algorithm we have developed in this study, shape sensing of snake robots with restricted available space can be achieved with high precision and much reduced cost.

## REFERENCES

[1] T. Ota, A. Degani, D. Schwartzman, B. Zubiate, J. McGarvey, H. Choset, and M. A. Zenati, "A highly articulated robotic surgical system for minimally invasive surgery," *The Annals of thoracic surgery*, vol. 87, no. 4, pp. 1253–1256, 2009.

[2] P. E. Dupont, J. Lock, B. Itkowitz, and E. Butler, "Design and control of concentric-tube robots," *Robotics, IEEE Transactions on*, vol. 26, no. 2, pp. 209–225, 2010.

[3] J. Shang, D. Noonan, C. Payne, J. Clark, M. Sodergren, A. Darzi, and G.-Z. Yang, "An articulated universal joint based flexible access robot for minimally invasive surgery," in *Robotics and Automation (ICRA), 2011 IEEE International Conference on*. IEEE, 2011, pp. 1147–1152.

[4] R. Buckingham and T. Francois, "Minimally invasive robots for confined spaces," *World Robotics Service Robots*, pp. 137–141, 2010.

[5] D. Vlasic, R. Adelsberger, G. Vannucci, J. Barnwell, M. Gross, W. Matusik, and J. Popović, "Practical motion capture in everyday surroundings," *ACM Transactions on Graphics (TOG)*, vol. 26, no. 3, p. 35, 2007.

[6] Z.-Q. Zhang, L.-Y. Ji, Z.-P. Huang, and J.-K. Wu, "Adaptive information fusion for human upper limb movement estimation," *Systems, Man and Cybernetics, Part A: Systems and Humans, IEEE Transactions on*, vol. 42, no. 5, pp. 1100–1108, 2012.

[7] Y. Xiaoping, E. R. Bachmann, and R. B. McGhee, "A simplified quaternion-based algorithm for orientation estimation from earth gravity and magnetic field measurements," *Instrumentation and Measurement, IEEE Transactions on*, vol. 57, no. 3, pp. 638–650, 2008.

[8] Z.-Q. Zhang, X.-L. Meng, and J.-K. Wu, "Quaternion-based kalman filter with vector selection for accurate orientation tracking," *Instrumentation and Measurement, IEEE Transactions on*, vol. 61, no. 10, pp. 2817–2824, 2012.

[9] D. Roetenberg, H. Luinge, and P. Slycke, "Xsens mvn: full 6DoF human motion tracking using miniature inertial sensors," *Xsens Motion Technologies BV, Tech. Rep*, 2009.

[10] Metamotion. IGS-190 motion capture system. [Online]. Available: http://www.metamotion.com/gypsy/gypsy-gyro.htm

[11] W. Y. Wong, M. S. Wong, and K. H. Lo, "Clinical applications of sensors for human posture and movement analysis: A review," *Prosthetics and orthotics international*, vol. 31, no. 1, pp. 62–75, 2007.

[12] S. Zhang, A. V. Rowlands, P. Murray, and T. Hurst, "Physical activity classification using the genea wrist-worn accelerometer," *Medicine and science in sports and exercise*, vol. 44, no. 4, pp. 742–748, 2012.

[13] X. Yun, J. Calusdian, E. R. Bachmann, and R. B. McGhee, "Estimation of human foot motion during normal walking using inertial and magnetic sensor measurements," *Instrumentation and Measurement, IEEE Transactions on*, vol. 61, no. 7, pp. 2059–2072, 2012.

[14] X. Meng, Z.-Q. Zhang, J.-K. Wu, and W.-C. Wong, "Hierarchical information fusion for global displacement estimation in microsensor motion capture," *Biomedical Engineering, IEEE Transactions on*, vol. 60, no. 7, pp. 2052–2063, 2013.

[15] H. Aldridge and J.-N. Juang, "Joint position sensor fault tolerance in robot systems using cartesian accelerometers," in *AIAA Guidance, Navigation, and Control Conference*, 1996.

[16] N. Miller, O. C. Jenkins, M. Kallmann, and M. J. Mataric, "Motion capture from inertial sensing for untethered humanoid teleoperation," in *Humanoid Robots, 2004 4th IEEE/RAS International Conference on*, vol. 2. IEEE, 2004, pp. 547–565.

[17] F. Ghassemi, S. Tafazoli, P. Lawrence, and K. Hashtrudi-Zaad, "An accelerometer-based joint angle sensor for heavy-duty manipulators," in *Robotics and Automation, 2002. Proceedings. ICRA'02. IEEE International Conference on*, vol. 2. IEEE, 2002, pp. 1771–1776.

[18] M. Quigley, R. Brewer, S. P. Soundararaj, V. Pradeep, Q. Le, and A. Y. Ng, "Low-cost accelerometers for robotic manipulator perception," in *Intelligent Robots and Systems (IROS), 2010 IEEE/RSJ International Conference on*. IEEE, 2010, pp. 6168–6174.

[19] P. Roan, N. Deshpande, Y. Wang, and B. Pitzer, "Manipulator state estimation with low cost accelerometers and gyroscopes," in *Intelligent Robots and Systems (IROS), 2012 IEEE/RSJ International Conference on*. IEEE, 2012, pp. 4822–4827.

[20] D. Choukroun, I. Bar-Itzhack, and Y. Oshman, "Novel quaternion Kalman filter," *IEEE Transactions on Aerospace and Electronic Systems*, vol. 42, no. 1, pp. 174–190, 2006.

[21] B. Lo and G. Yang, "Key technical challenges and current implementations of body sensor network," in *Proc. 2nd International Workshop on Body Sensor Networks (BSN 2005)*, 2005.

[22] A. D. ADXL330, http://www.analog.com/en/sensors/inertial-sensors/adxl330/products/product.html.

[23] I. ITG-3200, http://invensense.com/mems/gyro/itg3200.html.